Surface & Coatings Technology 205 (2010) S104–S108

Contents lists available at ScienceDirect

Surface & Coatings Technology

journal homepage: www.elsevier.com/locate/surfcoat

Nano-embossed structure on polypropylene induced by low energy Ar ion beam irradiation

Sk. Faruque Ahmed [a], Geon-Ho Rho [a], Ji Yeong Lee [b], Seong Jin Kim [c], Ho-Young Kim [c], Yong-Jun Jang [d], Myoung-Woon Moon [a,*], Kwang-Ryeol Lee [a]

[a] Convergence Technology Laboratory, Korea Institute of Science and Technology, P.O. Box 131, Cheongryang, Seoul 130-650, Republic of Korea
[b] Department of Nanoscience and Nanotechnology, Sungkyunkwan University, Suwon 440-746, Republic of Korea
[c] Division of Mechanical and Aerospace Engineering, Seoul National University, Seoul, 151-744, Republic of Korea
[d] Environment & Energy Research Team, Central Advanced Research & Engineering Institute for Hyundai Motor Company & Kia Motors Corporation, Gyeonggi-Do, Republic of Korea

ARTICLE INFO

Available online 8 June 2010

Keywords:
Polypropylene
Ar ion beam
Nanostructure
Hardness

ABSTRACT

The surface morphology evolution of polypropylene (PP) irradiated with an Ar ion beam was explored using a hybrid ion beam system. PP formed the emboss-like nanostructure of ~50 nm induced by the Ar ion beam treatment for shorter ion beam treatment times, while the emboss-like structure was transited into a 3-D long nanofiber-like nanostructure for longer treatment times. The Fourier transform infrared spectra revealed that the polymer chain cross-linking increased with increasing ion treatment time, while the Raman analysis showed that the conducting amorphous carbon increased on the surface of PP. The surface hardness and plane strain modulus of the PP decreased from 0.11 to 0.07 GPa and from 1.75 to 1.26 GPa, respectively, with respect to the Ar ion beam treatment time due to the surface nanostructures formed by the Ar ion beam.

1. Introduction

Surface treatment has been adopted to improve the important surface properties of polymers, such as adhesion, friction, wetting and biological compatibility, which are mainly influenced by the surface composition and structure rather than the bulk properties of the polymer. Also, the ability to fabricate nanostructures using surface treatment is essential in the development of devices that incorporate nanoscale functionality for mechanical, chemical and optical features [1–4]. The fabrication methods of the nanostructures on polymers have been developed in various ways including semiconductor processes such as a lithography and etch processes, embossing techniques with hot and UV embossing, nanoimprint lithography, soft lithography, and injection molding, and plasma/ion beam processes. Among these techniques, dry plasma/ion beam treatment processes have been developed in order to transform these inexpensive materials into highly valuable products [3,4]. Different plasmas have been used to modify the structural, mechanical, and chemical properties [5–7], but the interest has been more focused on Ar ion plasma because Ar is an inert gas and, therefore, does not chemically react with the organic surface.

The effects of Ar plasma on the wettability, surface chemistry and surface morphology of polymers, especially polypropylene, were studied [6]. The roughness and surface energy of polypropylene increased as a result of the Ar plasma treatment [6]. While Kwon et al. reported that the morphology of the PP film was different after the Ar/O_2 plasma treatment, the surface roughness was similar [7]. Formation of free radicals, recombination and scission of bonds, cross-linking, and the different oxidation reactions take place during ion the beam irradiation process on PP and are closely related to the different forms of radiation [4]. Therefore, the proper estimation of the structural and mechanical properties of PP is underway for further application of PP associated with the irradiation using Ar plasma or an ion beam.

However, no reports have discussed the detailed effects of the ion beam on the evolution of the emboss-like nanostructure of PP. This work examined the evolution of the surface morphology for the PP nanostructure and the change in the mechanical properties with increasing Ar ion treatment time at a low energy using a hybrid ion beam system. The PP used in this work was chosen because of its use in a variety of application fields such as aerospace, microelectronics, optoelectronics, composites and fiber optics due to its low cost, desirable mechanical properties, versatile electronic properties, good chemical resistance, biodegradability, easiness of processing and the absence of toxic byproducts [3,8,9]. Observation revealed that PP formed 3-D long fiber-like nanostructures at different ion exposure times. Alternations of the chemical bonds using ion irradiation was explored by chemical analysis and the observation of the ion beam treated surfaces, revealing that chain cross-linking in PP increased with increasing Ar ion treatment time. The decrease in the hardness and plain strain modulus of PP was explained in terms of the changes in the nanostructures induced by the Ar ion treatment.

* Corresponding author. Tel.: +82 2 958 5487; fax: +82 2 958 5509.
E-mail address: mwmoon@kist.re.kr (M.-W. Moon).

0257-8972/$ – see front matter © 2010 Elsevier B.V. All rights reserved.
doi:10.1016/j.surfcoat.2010.06.005

2. Experimental

The Ar ion beam treatment of PP (LG Chem) was carried out in a hybrid ion beam system. The sample coupons with dimensions of 10 mm × 10 mm × 2 mm were placed in the ion beam chamber, and the chamber was evacuated to a base pressure of 2×10^{-5} mbar. The distance between the ion source and the substrate holder was approximately 15 cm. Ar gas was introduced into the end-Hall type ion gun to obtain Ar ions with a flow rate of 8 sccm, and the anode voltage was kept at a constant value of 1 kV with a current density of 50 μA/cm^2. A radio frequency (r.f.) bias voltage was applied to the substrate holder at a bias voltage of −600 V and ion current of 44 mA. Ar ion beam was irradiated with exposure time varying from 5 to 50 min.

The surface morphology of the Ar ion beam treated PP was studied using a scanning electron microscope (SEM, NanoSEM, FEI Company) and an atomic force microscope (AFM, XE-70, Park Systems Corp.). To make direct observation of the cross-section of the nano-embossed pattern, the Ar PP treated for 50 min was explored using a dual-beam focused ion beam system (FIB, Nova 600, FEI). The chemical composition and bonding characteristics of the untreated as well as the Ar ion treated PP were analyzed using the Fourier transform infrared spectra (FTIR) spectra and the Raman spectra. The FTIR spectra were recorded using a FTIR spectrometer (FTIR, Infinity Gold FTIR, Thermo Mattson) in reflectance mode with a nominal resolution of 4 cm^{-1}, and the Raman measurements were made in a backscattering geometry with a Raman spectrometer (LabRAM HR, HORIBA Jobin-Yvon Inc.). A nanomechanical testing instrument (Triboindentor, Hysitron Inc.) was adopted to estimate the mechanical properties of the Ar ion beam treated PP surfaces. A Berkovich diamond tip with an approximate radius of curvature of 150 nm was used as the nanoindentation tip. Nanoindentation in the continuous stiffness measurement (CSM) mode was chosen to characterize the depth profiles of the hardness and elastic modulus of the PP with and without the Ar ion beam treatment. For four cases of Pristine PP, and 10, 30 and 50 min treated PP, nanoindentation was performed with a careful approach to the surface, followed by loading for 1 s, holding the indenter at a peak load for 0.5 s, unloading 90% of the peak load for 1 s, and holding the indenter after 90% unloading for 1 s. This cycle was continued until the maximum load of 150 μN was reached, and then the sample was unloaded completely. The single indentation mode was adopted in order to estimate the average values of the hardness and elastic modulus for each of the samples, Pristine PP, and 5, 10, 30 and 50 min treated PP. The load and displacement curves were recorded continuously up to a maximum load of 275 μN where the sample was loaded for 5 s, held for 5 s, and unloaded for 5 s. The hardness and plane strain modulus were evaluated from the load–displacement data using the well-known Oliver–Pharr method [10]. The measurement of the hardness and plane strain modulus was carried out at 6 different positions for each sample using indentation and calculated for the average value.

3. Results and discussion

3.1. Surface morphology studies

Fig. 1 shows the SEM images of the top view of the PP samples treated with the Ar ion beam for different irradiation times. The

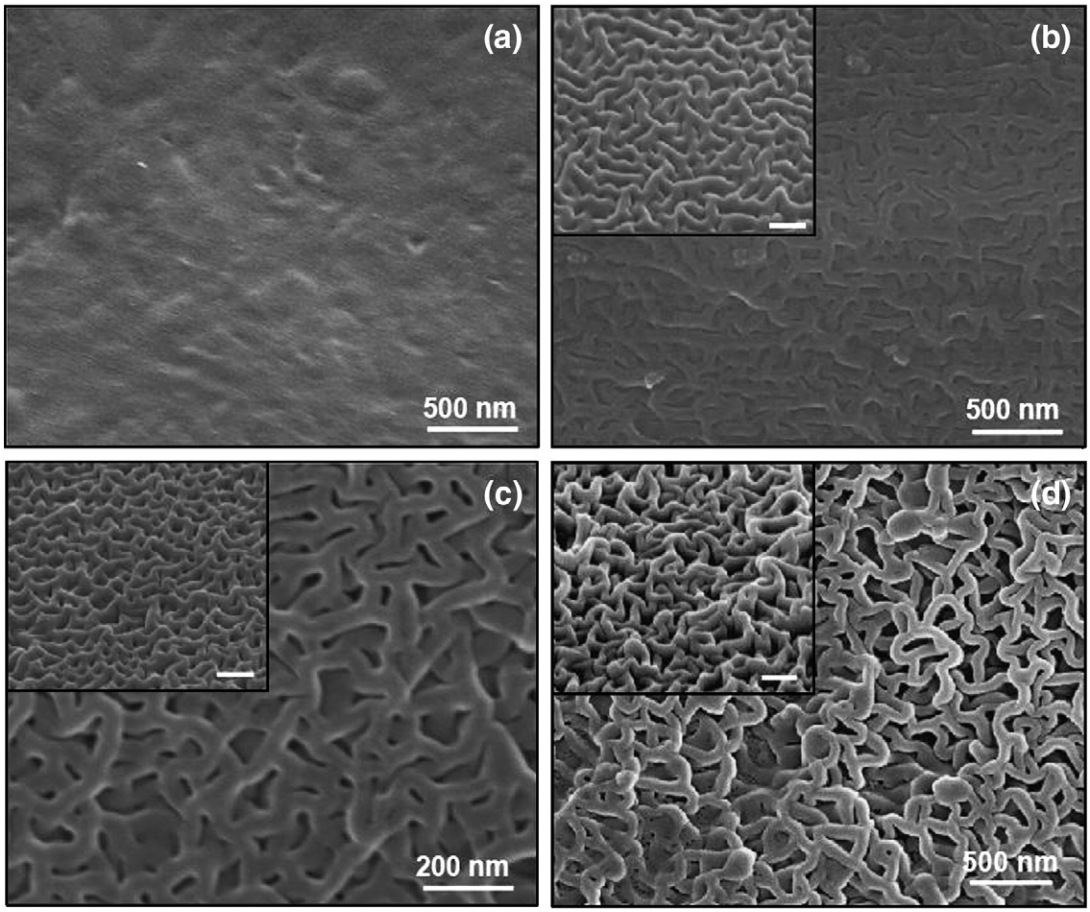

Fig. 1. SEM images of the PP surfaces (a) untreated, (b) 5 min, (c) 30 min and (d) 50 min treated with an Ar ion beam and the insets corresponding to the 50° tilted view. The length of the scale bar in the insets is 200 nm.

pristine PP substrate showed no specific pattern on the surface (Fig. 1(a)), while a certain fiber-like nanoscale pattern formed after 5 min of Ar ion beam irradiation in Fig. 1(b). Fig. 1(c) shows the emboss-like nanostructure of ~50 nm formed over the surface of the PP after the 30 min treatment, whereas PP formed 3-D long chain-like nanostructures i.e., nanofiber after 50 min of irradiation in Fig. 1(d). The morphology changed with increasing Ar ion treatment time even though the energy of the incident Ar ions was the same as the anode voltage of ion gun at 1 kV. The morphology induced by the noble gas plasma treatment was not only due to the ion species of the plasma but also depended on the total energy deposited by all of the species contained in the plasma and on the rate of the energy deposition [11]. The cross-sectional analysis in Fig. 2(a) and (b) revealed that the height of the nanofiber-like pattern formed after 50 min of Ar ion beam irradiation is measured as 80 nm which is relatively larger than the width of 50 nm. The AFM topography of the Ar ion beam treated PP surface after 30 min in Fig. 2(c) shows the root mean square (RMS) roughness, which increased with respect to the Ar ion treatment time in Fig. 2(d). These results were consistent with the report that stated that the roughness and surface energy of PP increased due to the low pressure Ar plasma treatment using radiofrequency discharge [6]. The Ar plasma treatment promoted the etching process and the impact of active species generated in Ar plasma, which increased the roughness with increasing treatment time in Fig. 2(d). Though different gases exhibit different etching rate of polymers, Ar was reported to be more powerful in roughening the surface through physical etching under the strong ion bombardment [12].

3.2. Chemical composition and boding analysis

The FTIR spectra of the Ar ion beam treated PP samples were analyzed at different treatment times in Fig. 3(a). The broad peaks at approximately 2950 cm^{-1} and 2920 cm^{-1} were assigned to the CH_3 and CH_2 asymmetric stretching modes, respectively, 2870–2880 cm^{-1} to the CH_3 and CH symmetric stretching, and 2836 cm^{-1} to the CH_2 asymmetric stretching vibration modes [13]. The prominent band was observed because of the symmetric and asymmetric vibrations of the methyl group near 1376 cm^{-1} and 1458 cm^{-1}, respectively, which were characteristic of PP [14]. The peak intensity at 1376 cm^{-1} increased with the treatment time due to the formation of additional CH_2 groups via radiation induced cross-linking mechanisms [14]. A broad absorption band between 1650 and 1720 cm^{-1}, assigned to the C O and C C stretching vibrations, was observed after the Ar ion beam treatment [13]. However, the most remarkable difference between the FTIR spectra before and after Ar treatment was seen in the region 2800–2950 cm^{-1} where the different CH_2 peaks increased as the Ar ion beam treatment time increased. Bhat et al. observed a similar effect during modification of PP with air, nitrogen, oxygen and ammonia plasma [13]. In general, scissioning and cross-linking occurred during irradiation of the polymer. Depending upon the type of radiation, dose rate and environment, either cross-linking or scissioning may dominate [7,13]. In

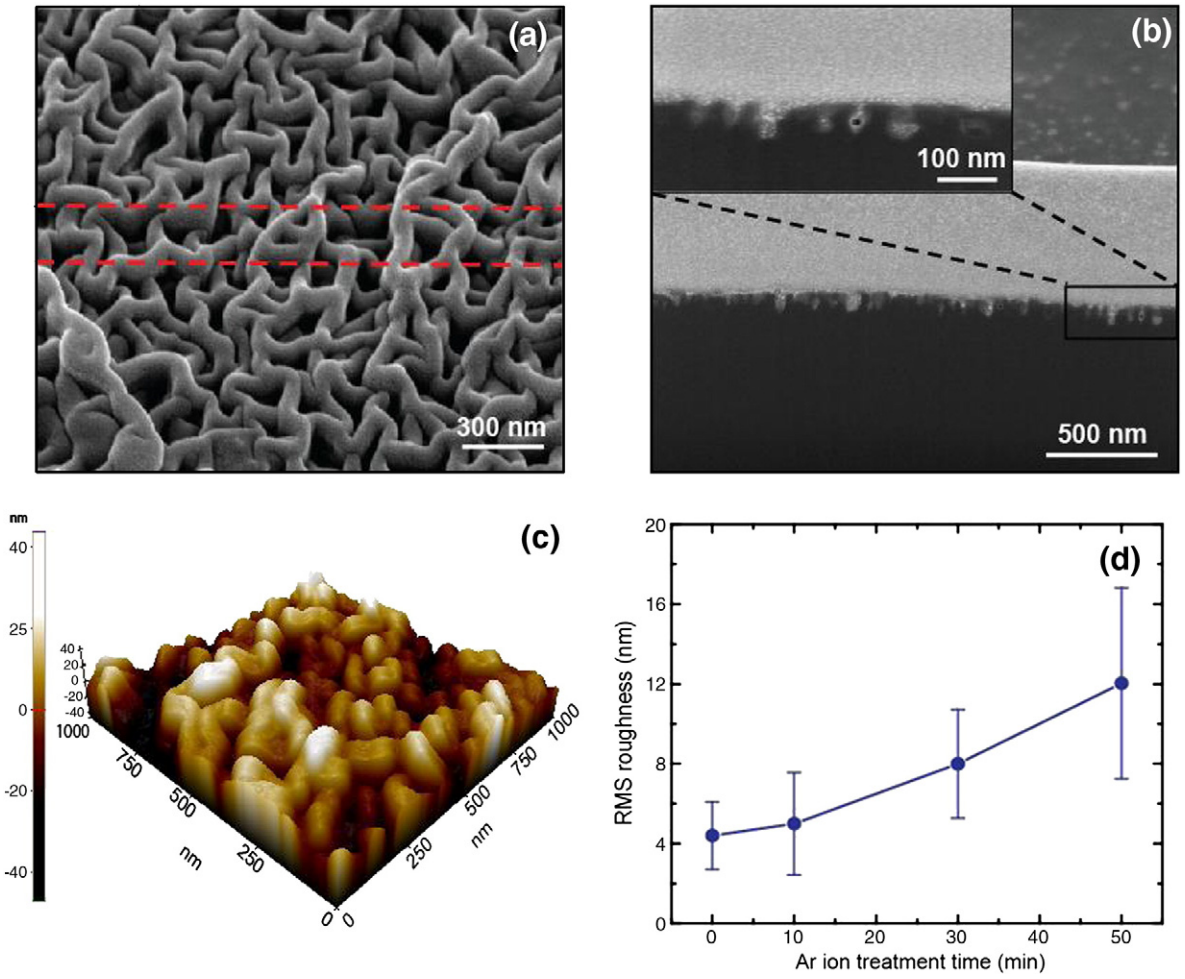

Fig. 2. (a) 50° tilted view SEM image of the PP surfaces treated Ar ion beam for 50 min, and (b) cross-sectional image sectioned on the red-dotted region of (a). (c) AFM images of the Ar ion beam treated PP surfaces with 30 min and (d) variation of the surface roughness with respect to the Ar ion beam treatment time.

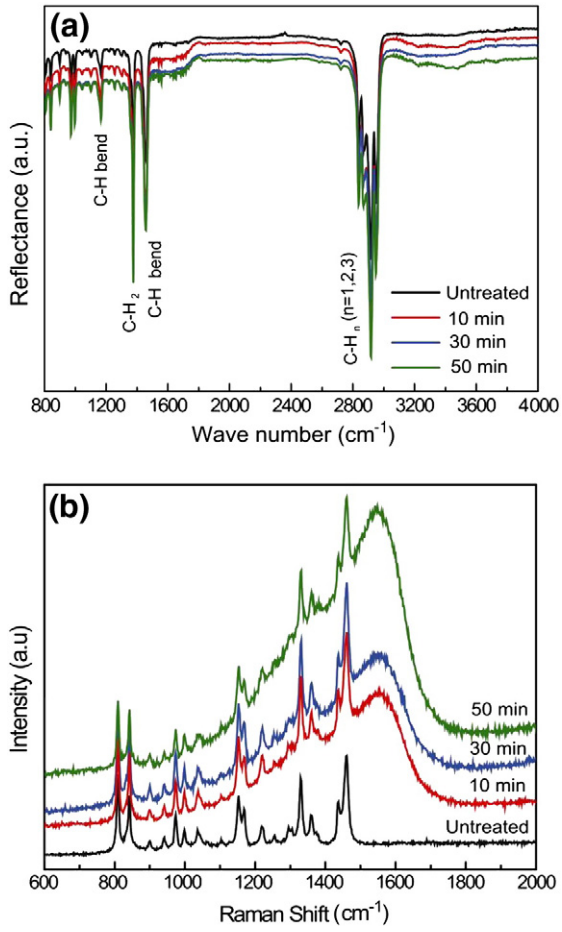

Fig. 3. (a) FTIR spectra and (b) Raman spectra of PP treated with respect to the Ar ion beam treatment time.

this case, the FTIR analysis also indicated that the amount of CH_3 groups decreased with increasing Ar ion treatment time and transformed into CH_2 groups inducing cross-linking in PP, which may be associated with the dominating nature of cross-linking over scissioning.

The Raman spectra of the Ar ion treated PP samples were measured at different treatment times in Fig. 3(b). The Raman peaks at 810, 842 and 1330 cm^{-1}, were assigned to the CH_2 rocking, C–C stretching and CH_2 twisting modes [15]. Several medium peaks decreased with treatment time such as the peak at 972 cm^{-1} for the asymmetric rocking CH_3 mixed with the CH_2 rocking and C–C stretching modes, 1154 cm^{-1} for the CH bending, and 1170 cm^{-1} for the CH_3 rocking and C–C wagging modes [16]. There was a significant change in the Raman spectra near 1200–1700 cm^{-1} after the Ar ion beam treatment on PP, and the broad dominant peak observed around 1200–1700 cm^{-1} increased with the Ar ion treatment time. In these Ar ion treated PP samples, a broad peak was observed in the region 1200–1700 cm^{-1} of the amorphous carbon materials, which exhibit two Raman modes known as the D (disorder graphitic) peak around 1365 cm^{-1} and the G (crystalline graphitic) peak around 1540 cm^{-1} [17]. The G mode has been observed at about 1535–1580 cm^{-1} in amorphous graphite (a-G) as well as in amorphous diamond (a-D, with a high degree of sp^3 hybridization) or at 1530–1550 cm^{-1} in sp^3 hybridized a-C:H [17]. The ion irradiation is known to produce a very high temperature (transient thermal spike) for a short time (~ pico-second) along the ion path. The high temperature generation along the ion path leads to the breaking of different bonds and the release of hydrogen from the polymer, which results in the chain-scission of the C–H bonds to form hydrogen free radicals that cross-link with each other [18]. The Raman analysis showed that amorphous carbon formed as an sp^2 and sp^3 hybridized mixture in the ion treated PP.

The high-energy ion irradiation induces ionization and excitation of the polymer molecules, which leads to different reactions between the excited and ionized species and creates more unsaturated sites involving conjugation or double bonds [18]. The Ar ion beam irradiation increased the formation of carbon double bonds (as confirmed by FTIR) and the carbon and hydrogen ratios and generated several carbon-enriched clusters in the polymer matrix (as confirmed by Raman analysis). The displacement of the target atoms through energetic collisions can cause permanent damage to the polymer, and the electronic excitation or the removal of valence electrons (ionization) can result in the formation of free radicals that may readily cross-link the polymer chains [19,20].

3.3. Mechanical properties

Fig. 4(a) and (b) show the change of the reduced modulus and hardness of the ion beam irradiated PP with respect to the indentation depth under the continuous stiffness measurement mode. For the Ar ion treated PP and the pristine PP, the hardness and plain strain modulus near the surface were higher than those below 100 nm due to roughness effect. The hardness of PP estimated with the continuous stiffness measurement mode increased near the surface due to roughness effect [21], and the hardness of the PET film increased due to the indentation size and crystallinity effect [22]. In Fig. 4(a) and (b), the hardness and modulus for the Ar ion treated PP barely changed until about 70 nm in penetration depth, which indicated that the ion beam affected the depth, while those for the pristine PP decreased gradually and became saturated. During the nanoindentation tests, the force (P) and displacement (h) curves in Fig 4(c) were obtained on the PP surfaces at different ion exposure times. The P–h curve indicated full elastic deformation in PP during indentation under this load condition. Increasing the Ar ion beam irradiation time increased the contact stiffness ($S = \mathrm{d}\,p/\mathrm{d}\,h$). Fig. 4(d) shows the relationship between the Ar ion beam treatment time and the hardness and plane strain modulus with a 275 μN load. The hardness of PP decreased from 0.11 to 0.07 GPa with increasing Ar treatment time, while the plain strain modulus decreased from 1.75 to 1.26 GPa. The estimated range for the hardness for the untreated PP was comparable to the PP thin film [23]. The results from both modes of the continuous stiffness measurement (Fig 4(a) and (b)) and the single stiffness measurement (Fig. 4(c) and (d)) were consistent for the behaviors of the hardness and plain strain modulus with respect to the Ar treatment time. The results in Fig. 4(d) suggested that the nanostructures evolved after Ar ion beam irradiation, which reduced the contact area against the indentation tip (see Fig. 1) and played a role in reducing the surface strength or hardness.

4. Conclusion

The morphological evolution and mechanical properties of the polypropylene surface were studied after Ar ion beam treatment from 5 to 50 min. SEM and AFM studies revealed that PP formed an emboss-like nanostructure of ~50 nm at the surface at lower Ar ion beam treatment times and 3-D long nanofiber-like nanostructures at higher treatment times. The chemical composition of the untreated and Ar ion treated PP was analyzed using the FTIR spectra and the Raman spectra. The FTIR analysis showed that the polymer chain cross-linking increased with increasing Ar ion beam treatment time, and the Raman analysis indicated that the conducting amorphous carbon increased on the surface of PP. The nanoindentation revealed that the surface hardness and plane strain modulus of the PP decreased from 0.11 to 0.07 GPa and from 1.75 to 1.26 GPa, respectively, as the Ar ion beam treatment time increased, which would be due to the surface nanostructures formed by the Ar ion beam.

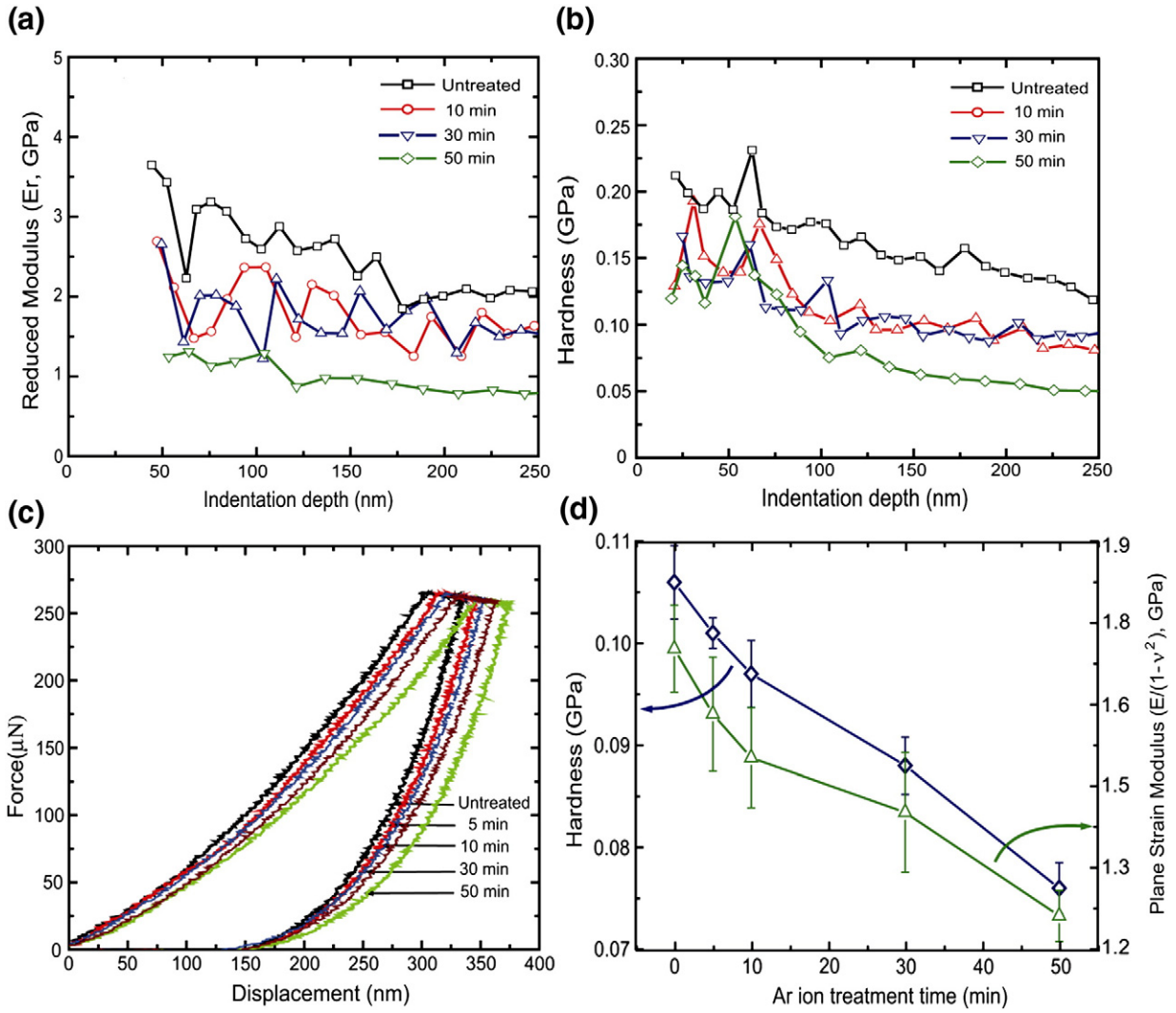

Fig. 4. Variation of the reduced modulus (a) and hardness (b) with respect to the indentation depth for the Ar ion treated PPs using the continuous stiffness measurement mode, (c) the force–displacement curve of the nanoindentation at an applied load of 275 mN and (d) change in the hardness and plain strain modulus of PP with respect to the Ar ion beam irradiation time.

Acknowledgments

This study was financially supported by a grant from the Hyundai Motor Company and Kia Motors Corporation (FA, MWM, KRL).

References

[1] P.W. Leech, R.A. Lee, Microelectron. Eng. 84 (2007) 25.
[2] S.F. Ahmed, J.W. Yi, M.W. Moon, Y.J. Jang, B.H. Park, S.H. Lee, K.R. Lee, Plasma Proc. Polym. 6 (2009) 860.
[3] R.L. Clough, Instrum. Meth. Phys. Res. B 185 (2001) 8.
[4] N. Spang, D. Theirich, J. Engemann, Surf. Coat. Technol. 74/75 (1995) 689.
[5] A.P. Kauling, G.V. Soares, C.A. Figueroa, R.V.B. Oliveira, I.J.R. Baumvol, C. Giacomelli, L. Miotti, Mater. Sci. Eng. C 29 (2009) 363.
[6] N. Gomathi, S. Neogi, Appl. Surf. Sci. 255 (2009) 7590.
[7] O.J. Kwon, S.W. Myung, C.S. Lee, H.S. Choi, J. Colloid Interface Sci. 295 (2006) 409.
[8] W.J. Kissel, J.H. Han, J.A. Meyer, in: H.G. Karian (Ed.), Handbook of Polypropylene and Polypropylene Composites, Taylor & Francis, New-York, 2003, p. 11.
[9] S. Zhang, A.R. Horrocks, Prog. Polym. Sci. 28 (2003) 1517.
[10] W.C. Oliver, G.M. Pharr, J. Mater. Res. 7 (6) (1992) 1564.
[11] M.C. Coen, G. Dietler, S. Kasas, P. Griining, Appl. Surf. Sci. 103 (1996) 27.
[12] S.M. Mirabedini, H. Arabi, A. Salem, S. Asiaban, Prog. Org. Coat. 60 (2007) 105.
[13] N. Bhat, D. Upadhyay, J. Appl. Polym. Sci. 86 (2002) 925.
[14] M.P. McDonald, I.M. Ward, Polymer 2 (1961) 341.
[15] H. Tadokoro, M. Kobayashi, M. Ukita, K. Yasufuku, S. Murahashi, J. Chem. Phys. 42 (1965) 1432.
[16] M.A.D. Baez, P.J. Hendra, M. Judkins, Spectrochim. Acta Part A 51 (1995) 2117.
[17] A.C. Ferrari, J. Robertson, Phys. Rev. B 61 (2000) 14095.
[18] W.L. Brown, Rad. Effects Def. Solids 98 (1986) 115.
[19] E.H. Lee, G.R. Rao, M.B. Lewis, C.K. Mansur, J. Mater. Res. 91 (1994) 1043.
[20] A. Chapiro, Radiation Chemistry of Polymer System, Interscience Publishers, London, 1962.
[21] S.H. Lee, S. Wang, G.M. Pharr, H. Xu, Compos. A 38 (2007) 1517.
[22] B.D. Beake, G.J. Leggett, Polymer 43 (2002) 319.
[23] G.R. Rao, E.H. Lee, L.K. Mansur, Wear 162–164 (1993) 739.